

Thermal Dehydrogenation Reaction of [N,N'-Bis(3-ethoxysalicylidene)-1,2-diphenyl-1,2-ethanediaminato]nickel(II) with [VO(salen)]NO₃ in the Solid State

Gakuse Hoshina, Masanobu Tsuchimoto, and Shigeru Ohba*

Department of Chemistry, Faculty of Science and Technology, Keio University, Hiyoshi 3-14-1, Kohoku-ku, Yokohama 223-8522

(Received August 2, 1999)

A dehydrogenation reaction of the red-brown powder of [Ni(3-EtOsalmeso-stien)] (H₂(3-EtOsalmeso-stien) = N,N'-bis(3-ethoxysalicylidene)-(R,S)(S,R)-1,2-diphenyl-1,2-ethanediamine) did not occur by heating solely in the air up to 210 °C. However, the reaction occurred upon heating together with [VO(salen)] (H₂(salen) = N,N'-disalicylidene-1,2-ethanediamine) in the air at 190 °C, and a red powder of [Ni(3-EtOsaltion)] (H₂(3-EtOsaltion) = N,N'-bis(3-ethoxysalicylidene)-1,2-diphenyl-1,2-ethenediamine) was obtained. The dehydrogenation reaction could also be carried out under Ar at 160 °C by mixing with [VO(salen)]NO₃. These facts revealed that the oxidants in solid state dehydrogenation in air are the V^V species originating from the V^{IV}=O complex. The crystal structures of [Ni(3-EtOsalmeso-stien)]·CH₃CN·H₂O, (1); [Ni(3-EtOsalmeso-stien)]·0.5H₂O, (2); and [Ni(3-EtOsaltion)]·CH₃OH·1.33H₂O, (3) were determined by X-ray analyses. [Ni(3-EtOsaltion)] was prepared in a dioxane solution of [Ni(3-EtOsalmeso-stien)] using DDQ (2,3-dichloro-5,6-dicyano-1,4-benzoquinone) as an oxidant. The *rac* complex, [Ni(3-EtOsalmeso-stien)] (H₂(3-EtOsalmeso-stien) = N,N'-bis(3-ethoxysalicylidene)-(R,R)(S,S)-1,2-diphenyl-1,2-ethanediamine), is less reactive in dehydrogenation than the *meso* in the solid state as well as in solution. The molecular structures in (1) and (2) indicate that the benzylic H atoms are sterically protected by phenyl groups in the *rac* complex, but are exposed to the oxidant in the *meso* complex.

Chiral Schiff-base complexes have attracted attention as catalysts for enantioselective reactions.¹ The oxovanadium(IV) complexes have catalytic properties for oxidation reactions.^{2,3} Recently, the authors found that [VO(Xsalmeso-stien)] (X is the substitute) complexes underwent thermal dehydrogenation in the solid state in the air to yield [VO(Xsaltion)].⁴ In the reaction, the two benzylic carbon atoms of the ligand were oxidized and a C=C double bond was formed. The dehydrogenation did not occur under an Ar atmosphere, but under oxygen. Therefore, it was obvious that oxygen was necessary for the reaction. However, the role of O₂ and that of the metal in the complex still remained unclear.

In order to further investigate the dehydrogenation reaction, nickel(II) complexes, [Ni(3-EtOsalmeso-stien)] and [Ni(3-EtOsalmeso-stien)], were prepared and examined in the present study. Dehydrogenation did not occur for [Ni(3-EtOsalmeso-stien)], but it gave a clue that led to reveal the reaction mechanism. The nickel(II) complex could be dehydrogenated by heating with [VO(salen)] in the air, even in an Ar atmosphere by heating with [VO(salen)]NO₃ (Fig. 1). The oxidation reaction of the nickel(II) complex in a dioxane solution was also examined by using DDQ as an oxidant. The reactivities of *meso*- and *rac*-[Ni(3-EtOsalmeso-stien)] were much different, indicating some geometrical requirement for dehydrogenation. X-Ray structure analyses of (1), (2), and (3) were carried out to investigate the molecular conforma-

tions of *meso* and *rac* complexes, and to confirm the structure of the dehydrogenation product.

Experimental

Schiff-base oxovanadium complexes [VO(salen)], [VO(salen)]NO₃, and *exo*-[VO(3-EtOsalmeso-stien)] and the ligands H₂(3-EtOsalmeso-stien) and H₂(3-EtOsalmeso-stien) were prepared according to reported procedure.^{3,4} High-performance liquid-chromatography (HPLC) was carried out with a Shimadzu LC-10AD pumping unit and a Shimpack CLC-ODS column (eluent: CH₃CN–H₂O (8:2 v/v)). The components of the chromatography were detected with a Shimadzu SPD-10A UV-vis detector at 250 nm. The ¹H NMR spectra were recorded at 26 °C on a JEOL JNM-EX270 and referred to tetramethylsilane as an internal standard. UV-vis spectra were recorded on a JASCO V-570 spectrophotometer.

Synthesis of [Ni(3-EtOsalmeso-stien)]. [Ni(3-EtOsalmeso-stien)] was prepared by the reaction of a hot methanol solution (50

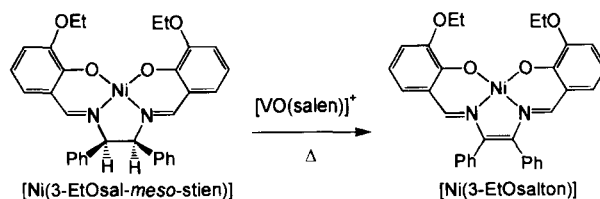


Fig. 1. Thermal dehydrogenation of [Ni(3-EtOsalmeso-stien)] by [VO(salen)]⁺ in the solid state.

ml) of nickel(II) acetate tetrahydrate (0.996 g, 4 mmol) with H₂(3-EtOsai-*meso*-stien) (2.034 g, 4 mmol). The resulting red-brown precipitate was collected by filtration and washed with ether. Yield of [Ni(3-EtOsai-*meso*-stien)]: 1.86 g (82%). Found: C, 68.21; H, 5.24; N, 5.06%. Calcd for C₃₂H₃₀N₂NiO₄: C, 67.99; H, 5.35; N, 4.96%. ¹H NMR (CDCl₃) δ = 1.48 (t, J = 7.01 Hz, 6H), 4.06 (m, 4H), 5.18 (s, 2H), 6.20 (m, 4H), 6.63 (dd, J = 6.84, 2.06 Hz, 2H), 6.79 (s, 2H), 7.16 (m, 6H), 7.42 (br, 4H). UV-vis (DMSO; DMSO = dimethyl sulfoxide) $\sigma_{\text{max}}/10^3 \text{ cm}^{-1}$ (log ($\epsilon/\text{mol}^{-1} \text{ dm}^3 \text{ cm}^{-1}$)) 17.2 (sh), 21.5 (sh), 23.6 (3.69), 28.1 (3.82), 38.1 (4.62). Red-brown crystals of [Ni(3-EtOsai-*meso*-stien)]·CH₃CN·H₂O (**1**) were grown by slow evaporation of an acetonitrile solution.

Synthesis of [Ni(3-EtOsai-*rac*-stien)]. The *rac* complex was prepared similarly as described above for [Ni(3-EtOsai-*meso*-stien)]. Yield of [Ni(3-EtOsai-*rac*-stien)]: 1.76 g (78%). Found: C, 67.99; H, 5.24; N, 4.95%. Calcd for C₃₂H₃₀N₂NiO₄: C, 67.99; H, 5.35; N, 4.96%. ¹H NMR (CDCl₃) δ = 1.50 (t, J = 6.92 Hz, 6H), 4.03 (q, J = 6.92 Hz, 4H), 4.46 (s, 2H), 6.37 (m, 2H), 6.56 (d, J = 6.92 Hz, 2H), 6.69 (d, J = 6.60 Hz, 2H), 7.35 (m, 8H), 7.97 (d, J = 7.26 Hz, 4H). Red-brown crystals of [Ni(3-EtOsai-*rac*-stien)]·0.5H₂O (**2**) were grown by slow evaporation of an acetonitrile solution.

Synthesis of [Ni(3-EtOsai-*rac*-stien)]. To a dioxane solution (40 ml) of DDQ (0.272 g, 1.2 mmol) was added [Ni(3-EtOsai-*meso*-stien)] (0.565 g, 1 mmol), and the solution was refluxed for 15 h. The undissolved byproduct was removed by filtration, and the filtrate was evaporated to dryness. After the residue was suspended in methanol, slightly soluble [Ni(3-EtOsai-*rac*-stien)] was collected by filtration as a solid and washed with ethanol and diethyl ether. Yield of [Ni(3-EtOsai-*rac*-stien)]·H₂O: 0.406 g (72%). Found: C, 66.42; H, 4.88; N, 5.09%. Calcd for C₃₂H₂₈N₂NiO₄: C, 66.12; H, 5.20; N, 4.82%. ¹H NMR (CDCl₃) δ = 1.56 (t, J = 6.93 Hz, 6H), 4.10 (q, J = 6.93 Hz, 4H), 6.47 (m, 2H), 6.63 (d, J = 6.92 Hz, 2H), 6.75 (d, J = 7.59 Hz, 2H), 7.10 (m, 4H), 7.29 (m, 6H), 7.38 (s, 2H). UV-vis

(DMSO) $\sigma_{\text{max}}/10^3 \text{ cm}^{-1}$ (log ($\epsilon/\text{mol}^{-1} \text{ dm}^3 \text{ cm}^{-1}$)), 17.4(sh), 19.9 (3.75), 26.3 (4.25), 33.7(4.01), 38.3 (4.56). Red crystals of [Ni(3-EtOsai-*rac*-stien)]·CH₃OH·1.33H₂O (**3**) were grown by slow evaporation of a dichloromethane-methanol (1 : 1 v/v) solution.

Crystal Structure Determination. The X-ray intensities were measured at 25 °C with graphite-monochromatized Mo $K\alpha$ radiation (λ = 0.71073 Å) up to 2θ = 55° on a Rigaku AFC-5 diffractometer for **1** and **3**, and on a Rigaku AFC-7R diffractometer for **2**. The crystal data and the experimental details are given in Table 1. Although the crystals were coated with an adhesive to prevent efflorescence, the intensities of the standard reflections for **1** decreased by 23%, which was corrected. The absorption effect was corrected by a numerical-integration method based on the crystal shape. The structures were solved by direct methods and refined using TEXSAN software⁵ for **1** and **2**, and SHELXL-97⁶ for **3**. Hydrogen atoms were introduced at ideal positions, except for the solvent molecules for crystallization. Large displacement parameters for one of the ethoxy substituents in **2** may be due to a positional disorder. The site occupation factor of O40 (water for crystallization) in **2** was estimated to be 50% based on the thermal parameters. In **3**, the water O40 atom has a site occupation factor of 100%. The other water molecules are disordered around the $\bar{3}$ symmetry center. Selected geometrical parameters are listed in Table 2. The atomic coordinates, thermal parameters, bond distances and bond angles, and $F_o - F_c$ tables are deposited as Document No. 73010 at the Office of the Editor of Bull. Chem. Soc. Jpn. Crystallographic data have been deposited at the CCDC, 12 Union Road, Cambridge CB2 1EZ, UK and copies can be obtained on request, free of charge, by quoting the publication citation and the deposition numbers 136493-136495.

Thermal Dehydrogenation in the Solid State. The reactivity of the nickel(II) complex was examined under the conditions listed in the first half of Table 3. For example, in Entry 2, the powder of [Ni(3-EtOsai-*meso*-stien)] and two equivalent amounts of [VO-

Table 1. Crystallographic Data for [Ni(3-EtOsai-*meso*-stien)]·CH₃CN·H₂O (**1**), [Ni(3-EtOsai-*rac*-stien)]·0.5H₂O (**2**), and [Ni(3-EtOsai-*rac*-stien)]·CH₃OH·1.33H₂O (**3**)

	1	2	3
Formula	C ₃₄ H ₃₅ N ₃ NiO ₅	C ₃₂ H ₃₁ N ₂ NiO _{4.5}	C ₃₃ H _{34.67} N ₂ NiO _{6.33}
F.W.	624.37	574.31	619.30
Crystal size/mm	0.6 × 0.6 × 0.6	0.3 × 0.3 × 0.2	0.7 × 0.5 × 0.3
Crystal system	Monoclinic	Orthorhombic	Trigonal
Space group	$P2_1/c$	$Fdd2$	$R\bar{3}$
$a/\text{\AA}$	15.170(3)	25.815(6)	31.227(8)
$b/\text{\AA}$	13.420(3)	33.826(8)	31.227
$c/\text{\AA}$	16.633(2)	12.563(6)	16.343(10)
$\beta/^\circ$	112.659(9)	—	—
$V/\text{\AA}^3$	3124.7(8)	10969(5)	13801(10)
Z	4	16	18
$D_{\text{calc}}/\text{Mg cm}^{-3}$	1.327	1.391	1.348
$\mu(\text{Mo } K\alpha)/\text{mm}^{-1}$	0.67	0.75	0.68
No. of reflections ^{a)}	7166	3293	3281
No. of parameters	388	362	388
$R(I > 2\sigma)^b$	0.048	0.042	0.071
R_w^c	0.056	0.070	0.205
S	1.54	1.05	0.96

a) $|F_o| > 3\sigma(|F_o|)$. b) $R = \sum ||F_o| - |F_c|| / \sum |F_o|$ for **1** and **2**. $R = \sum |F_o^2 - F_c^2| / \sum F_o^2$ for **3**. c) $R_w = [\sum w(|F_o| - |F_c|)^2 / \sum w|F_o|^2]^{1/2}$ for **1** and **2**, $w^{-1} = \sigma^2(F_o) + 0.0002|F_o|^2$ for **1**, $w^{-1} = \sigma^2(F_o) + 0.0024|F_o|^2$ for **2**, $R_w = [\sum w(F_o^2 - F_c^2)^2 / \sum w(F_o^2)^2]^{1/2}$, $w^{-1} = \sigma^2(F_o^2) + (0.1000P)^2$ where $P = (F_o^2 + 2F_c^2)/3$ for **3**.

Table 2. Selected Bond Lengths (\AA), Bond Angles ($^\circ$) and Torsional Angles ($^\circ$) of $[\text{Ni}(\text{3-EtOs}al\text{-}meso\text{-stien})]\cdot\text{CH}_3\text{CN}\cdot\text{H}_2\text{O}$ (1), $[\text{Ni}(\text{3-EtOs}al\text{-}rac\text{-stien})]\cdot 0.5\text{H}_2\text{O}$ (2), and $[\text{Ni}(\text{3-EtOs}al\text{-}salton)]\cdot\text{CH}_3\text{OH}\cdot 1.33\text{H}_2\text{O}$ (3)

	1	2	3
Ni1–O2	1.847(2)	1.857(4)	1.849(4)
Ni1–O3	1.841(2)	1.849(4)	1.851(4)
Ni1–N6	1.839(2)	1.851(4)	1.846(4)
Ni1–N7	1.856(2)	1.847(4)	1.854(4)
C17–C24	1.539(4)	1.532(8)	1.336(7)
O2–Ni1–O3	84.77(8)	84.8(2)	85.2(2)
N6–Ni1–N7	86.2(1)	86.8(2)	85.4(2)
Ni1–N6–C17–C18	–88.6(3)	–157.6(4)	–172.9(5)
Ni1–N7–C24–C25	155.6(2)	–147.3(4)	169.3(5)
N6–C17–C24–N7	–38.8(3)	33.2(5)	1.3(8)
C18–C17–C24–C25	–45.0(3)	–75.1(5)	3(1)
H17–C17–C24–H24	–41	163	—

(salen)] were mixed in a mortar with a pestle. The mixture was heated at 190°C for 17 h in the air. The conversion of $[\text{Ni}(\text{3-EtOs}al\text{-}meso\text{-stien})]$ into $[\text{Ni}(\text{3-EtOs}al\text{-}salton)]$ was measured by the HPLC method with acetonitrile–water (8 : 2 v/v) as an eluent. In Entries 3 and 4 of Table 3, a powdered mixture of $[\text{Ni}(\text{3-EtOs}al\text{-}meso\text{-stien})]$ and two equivalent amounts of $[\text{VO}(\text{salen})]$ or $[\text{VO}(\text{salen})]\text{NO}_3$ was heated at 160°C for 50 h in the air.

The reactivity of the oxovanadium(IV) complex, *exo*- $[\text{VO}(\text{3-EtOs}al\text{-}meso\text{-stien})]$, was also examined under the conditions listed in the second half of Table 3. In Entry 12, a powdered mixture of $[\text{VO}(\text{3-EtOs}al\text{-}meso\text{-stien})]$ and two equivalent amounts of $[\text{VO}(\text{salen})]\text{NO}_3$ were heated at 160°C for 50 h under Ar. The conversion of $[\text{VO}(\text{3-EtOs}al\text{-}meso\text{-stien})]$ into $[\text{VO}(\text{3-EtOs}al\text{-}salton)]$ was measured with a HPLC method with acetonitrile–water (8 : 2 v/v) used as an eluent.

Dehydrogenation Reaction in Solution. To a dioxane solution (100 ml) of DDQ (0.068 g, 0.3 mmol) was added *meso* or *rac*- $[\text{Ni}(\text{3-EtOs}al\text{-}stien)]$ (0.057 g, 0.1 mmol); the solution was kept at 100°C .

The progress of the reaction was followed by the HPLC method at constant intervals.

Results and Discussion

Synthesis. Brown nickel(II) complexes with Schiff-base ligands 3-EtOs*al-meso*-stien and 3-EtOs*al-rac*-stien were prepared. These square-planar nickel(II) complexes were practically diamagnetic, and were characterized by the ^1H NMR spectra. The 3-EtO substituted stien ligands were selected because of easy crystallization of the metal complexes for an X-ray study. Although $[\text{Ni}(\text{3-EtOs}al\text{-}salton)]$ was obtained by heating together with $[\text{VO}(\text{salen})]$ in the solid state, purification was rather difficult. Separately, the salton complex was prepared in moderate yield in a dioxane solution of $[\text{Ni}(\text{3-EtOs}al\text{-}stien)]$ by using DDQ as an oxidant. In the process of dehydrogenation by DDQ, light-yellow DDH (2,3-dichloro-5,6-dicyano-1,4-dihydroxybenzene) was produced. It is worth noting that one may obtain not only crystals of the nickel(II) complex and those of DDH, but also red crystals in which the nickel(II) complex and DDH are stacked alternately.⁷

The electronic spectra show that the charge-transfer bands of $[\text{Ni}(\text{3-EtOs}al\text{-}salton)]$ are shifted to lower energy than those of $[\text{Ni}(\text{3-EtOs}al\text{-}meso\text{-stien})]$ (Fig. 2). This may be due to a long conjugated π -system of the salton ligand. The shoulder in the absorption spectra of $[\text{Ni}(\text{3-EtOs}al\text{-}meso\text{-stien})]$ at 17200 cm^{-1} is a d–d band, which is hidden by a charge-transfer band around 17400 cm^{-1} for $[\text{Ni}(\text{3-EtOs}al\text{-}salton)]$.

X-Ray Crystal Structures of $[\text{Ni}(\text{3-EtOs}al\text{-}meso\text{-stien})]\cdot\text{CH}_3\text{CN}\cdot\text{H}_2\text{O}$ (1), $[\text{Ni}(\text{3-EtOs}al\text{-}rac\text{-stien})]\cdot 0.5\text{H}_2\text{O}$ (2), and $[\text{Ni}(\text{3-EtOs}al\text{-}salton)]\cdot\text{CH}_3\text{OH}\cdot 1.33\text{H}_2\text{O}$ (3). The molecular structures of the nickel(II) complexes in 1, 2, and 3 are shown in Figs. 3, 4, and 5. Selected bond lengths, bond angles and torsion angles are listed in Table 2. Although the coordination geometry around nickel is approximately square planar, there is a slight tetrahedral distortion. The

Table 3. Reactivity of $[\text{Ni}(\text{3-EtOs}al\text{-}stien)]$ and $[\text{VO}(\text{3-EtOs}al\text{-}stien)]$ in the Solid State

Entry	Complex	Oxidant ^{a)}	Atmosphere	Temperature	Time	Conversion ^{b)}
				$^\circ\text{C}$	h	%
1	$[\text{Ni}(\text{3-EtOs}al\text{-}meso\text{-stien})]$	—	Air	210	15	0
2	$[\text{Ni}(\text{3-EtOs}al\text{-}meso\text{-stien})]$	$[\text{VO}(\text{salen})]$	Air	190	17	24
3	$[\text{Ni}(\text{3-EtOs}al\text{-}meso\text{-stien})]$	$[\text{VO}(\text{salen})]$	Air	160	50	10
4	$[\text{Ni}(\text{3-EtOs}al\text{-}meso\text{-stien})]$	$[\text{VO}(\text{salen})]\text{NO}_3$	Air	160	50	56
5	$[\text{Ni}(\text{3-EtOs}al\text{-}meso\text{-stien})]$	$[\text{VO}(\text{salen})]$	Ar	190	17	0
6	$[\text{Ni}(\text{3-EtOs}al\text{-}meso\text{-stien})]$	$[\text{VO}(\text{salen})]\text{NO}_3$	Ar	160	50	54
7	$[\text{Ni}(\text{3-EtOs}al\text{-}rac\text{-stien})]$	$[\text{VO}(\text{salen})]$	Air	190	17	2
8	$[\text{Ni}(\text{3-EtOs}al\text{-}rac\text{-stien})]$	$[\text{VO}(\text{salen})]\text{NO}_3$	Ar	160	50	3
9	<i>exo</i> - $[\text{VO}(\text{3-EtOs}al\text{-}meso\text{-stien})]$	—	Ar	210	15	0
10	<i>exo</i> - $[\text{VO}(\text{3-EtOs}al\text{-}meso\text{-stien})]$	—	Air	190	17	60
11	<i>exo</i> - $[\text{VO}(\text{3-EtOs}al\text{-}meso\text{-stien})]$	—	Air	160	50	31
12	<i>exo</i> - $[\text{VO}(\text{3-EtOs}al\text{-}meso\text{-stien})]$	$[\text{VO}(\text{salen})]\text{NO}_3$	Ar	160	50	89
13	$[\text{VO}(\text{3-EtOs}al\text{-}rac\text{-stien})]$	—	Air	190	17	5
14	$[\text{VO}(\text{3-EtOs}al\text{-}rac\text{-stien})]$	$[\text{VO}(\text{salen})]\text{NO}_3$	Ar	160	50	7

a) complex : oxidant = 1 : 2. b) $100 [\text{M}(\text{3-EtOs}al\text{-}salton)] / \{ [\text{M}(\text{3-EtOs}al\text{-}stien)] + [\text{M}(\text{3-EtOs}al\text{-}salton)] \}$. M = Ni for Entries 1–8; VO for Entries 9–14.

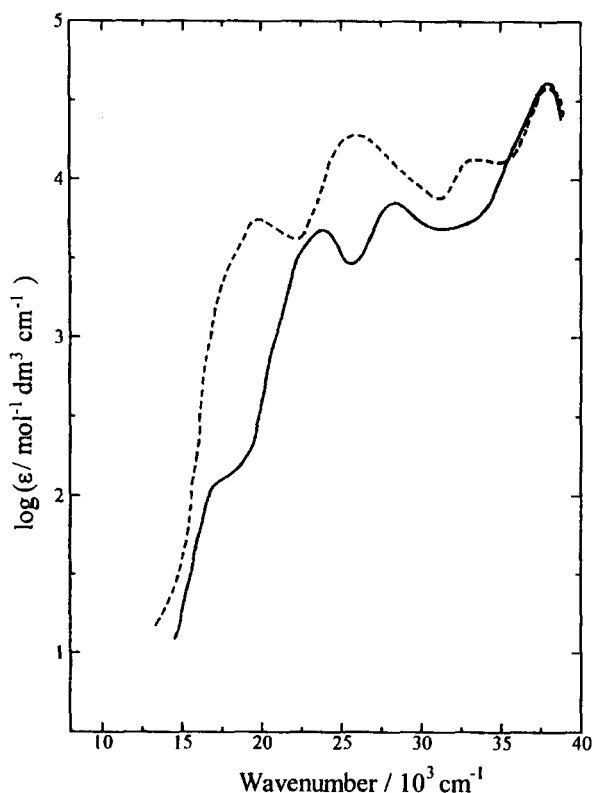


Fig. 2. Electronic spectra of $[\text{Ni}(\text{3-EtOsalmeso-stien})]$ (—) and $[\text{Ni}(\text{3-EtOsaltion})]$ (---) in DMSO solution.

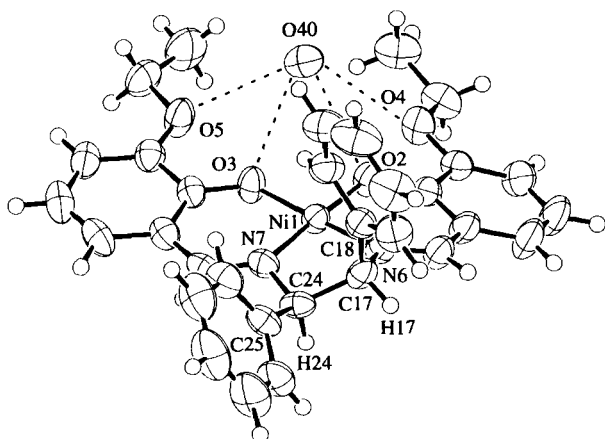


Fig. 3. Molecular structure of $[\text{Ni}(\text{3-EtOsalmeso-stien})]$ in **1**. The displacement ellipsoids are at 50% probability level. The O40 is a water of crystallization, and hydrogen bonds are indicated with broken lines.

dihedral angles between the O2–Ni1–N6 and O3–Ni1–N7 planes are 4.8(1), 3.3(2), and 1.9(2)° for **1**, **2**, and **3**, respectively. The five-membered N–N chelate ring in **1** and **2** takes a distorted gauche conformation with two benzylic H17 and H24 atoms located on the same side of the coordination plane in **1**, and the opposite side in **2**. The orientation of two phenyl groups are axial and equatorial (*ax eq*) for the *meso* complex in **1**, and *eq₂* for the *rac* complex in **2**. In **3**, the five-membered chelate ring of the saltion complex is almost flat and the C–Ph bond axes lie nearly on the coordination plane (Fig. 5).

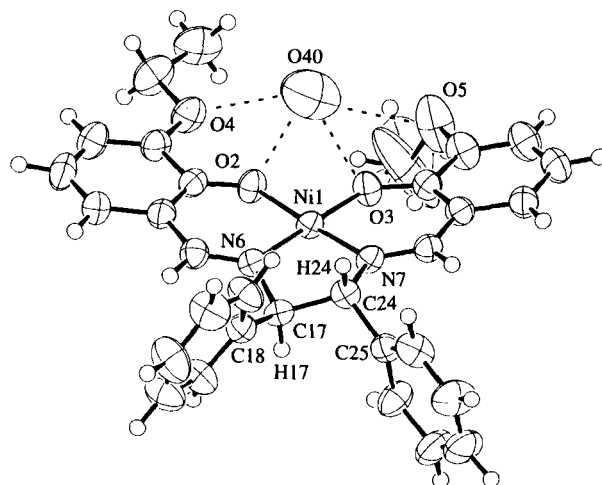


Fig. 4. Molecular structure of $[\text{Ni}(\text{3-EtOsaltion})]$ in **2**. The displacement ellipsoids are at 50% probability level. The O40 is a water of crystallization, and hydrogen bonds are indicated with broken lines.

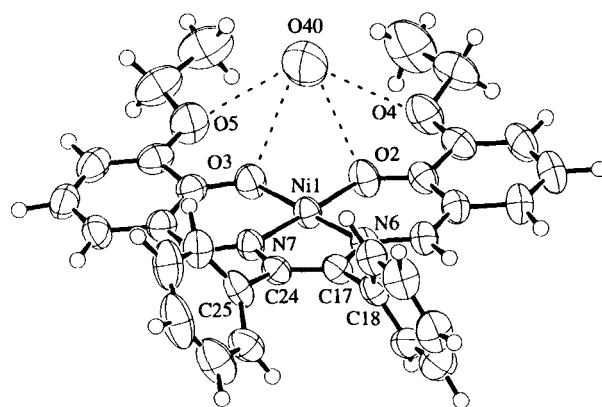


Fig. 5. Molecular structure of $[\text{Ni}(\text{3-EtOsaltion})]$ in **3**. The displacement ellipsoids are at 50% probability level. The O40 is a water of crystallization, and hydrogen bonds are indicated with broken lines.

In each crystal, the water molecule for crystallization (O40) is surrounded by four oxygen atoms of the ligand (O2, O3, O4, O5) with O···O distances of 2.71(2)–3.127(3) Å. The O40 atom is shifted from the O₄ best plane by 1.634(3) Å in **1**, 0.28(3) Å in **2**, and 1.53(1) Å in **3**. Difference syntheses suggested that two H atoms of O40 lie between O3 and O5, and between O2 and O4 to form bifurcated hydrogen bonds. A similar structural feature concerning the encapsulation of a water molecule with two ethoxy substituents at the 3-positions was reported for Schiff-base oxovanadium(IV) complexes.^{3,8–10}

Thermal Dehydrogenation in the Solid State. The results of dehydrogenation experiments of $[\text{Ni}(\text{3-EtOsaltion})]$ in the solid state are listed in the first half of Table 3. When a powder of $[\text{Ni}(\text{3-EtOsalmeso-stien})]$ was solely heated at 210 °C in the air (Entry 1), the dehydrogenation reaction did not occur. When the powder was mixed with $[\text{VO}(\text{salen})]$ and heated in the air (Entries 2 and 3), $[\text{Ni}(\text{3-EtOsaltion})]$ was obtained (conversion 24% after 17 h at 190 °C, and 10%

after 50 h at 160 °C). When the powder was mixed with [VO(salen)]NO₃ and heated at 160 °C in the air (Entry 4), the conversion was 56% after 50 h. The dehydrogenation reaction with [V^{VO}(salen)]NO₃ proceeded even under an Ar atmosphere (Entry 6, conversion 54%), but the reaction with [V^{IV}O(salen)] did not occur under Ar at 190 °C (Entry 5). These facts indicate that the nickel complexes are oxidized by [V^{VO}O(salen)]⁺. [V^{VO}O(salen)]⁺ may be produced from [V^{IV}O(salen)] with oxygen in the air upon heating.

Compared with the *meso* complex, the *rac* complex [Ni(3-EtOsAl-*rac*-stien)] was less dehydrogenated by [VO(salen)]⁺ in the solid state (Entries 7 and 8 in Table 3; conversion 2–3%). The H atoms at the benzylic carbons are sterically protected by phenyl groups in the *rac* complex, but are exposed to the oxidant in the *meso* complex (Figs. 3 and 4). Therefore, the geometrical structure of the *meso* complex is preferable for dehydrogenation.

The authors have reported that the thermal dehydrogenation of *exo*-[VO(Xsal-*meso*-stien)] (X = 3-EtO, 5-MeO, 5-Br) occurred in the air, but not in Ar, and that the reaction occurred in O₂.³ However, the present study on the nickel(II) complex revealed that O₂ was not a direct oxidant. The results of dehydrogenation experiments of *exo*-[VO(3-EtOsAlstien)] in the solid state are listed in the second half of Table 3. Although the reaction did not occur at 210 °C under Ar (Entry 9), the dehydrogenation reaction occurred by mixing with [VO(salen)]NO₃ and heating at 160 °C under Ar (Entry 12, conversion 89%). This fact suggests that the dehydrogenation of oxovanadium(IV) complexes in the air (Entries 10 and 11) occurred by V^V species originated from the V^{IV}=O complex and O₂. There are two possible geometrical isomers, *endo* and *exo*, for [VO(3-EtOsAl-*meso*-stien)], and the *exo* isomer (two benzylic H atoms oriented apart from the V=O bond) is thermodynamically more stable than the *endo* isomer in the solid state.¹⁰ The *exo*-[VO(3-EtOsAl-*meso*-stien)] is more reactive in thermal dehydrogenation than [VO(3-EtOsAl-*rac*-stien)] (Entries 13 and 14), indicating again the preferability of the *cis* configuration of the two benzylic H atoms.³

Dehydrogenation by DDQ in Solution. The dehydrogenation reactions of *meso* and *rac*-[Ni(3-EtOsAlstien)] by DDQ in a dioxane solution at 100 °C were followed by HPLC measurements (Fig. 6). The *rac* complex was less reactive than the *meso* complex. In 10 h, the reaction completed for the *meso* complex, but the conversion of the *rac* complex was only 28%. This fact indicates that the *cis* configuration of two benzylic hydrogen atoms in [Ni(3-EtOsAl-*meso*-stien)] is preferable for an intermolecular oxidation reaction with DDQ in solution as well as with [VO(salen)]⁺ in the solid state.

In the solution, a dynamical change in the molecular conformation is expected. As shown in Fig. 7, the packing motion of the five-membered N–N chelate ring changed the two phenyl orientations from *eq*₂ to *ax*₂ for the *rac* complex (*trans* benzylic H atoms), but from *eq* *ax* to *ax* *eq* (just the mirror image of *eq* *ax*) for the *meso* complex (*cis* H atoms). The benzylic H atoms are sterically protected by the phenyl

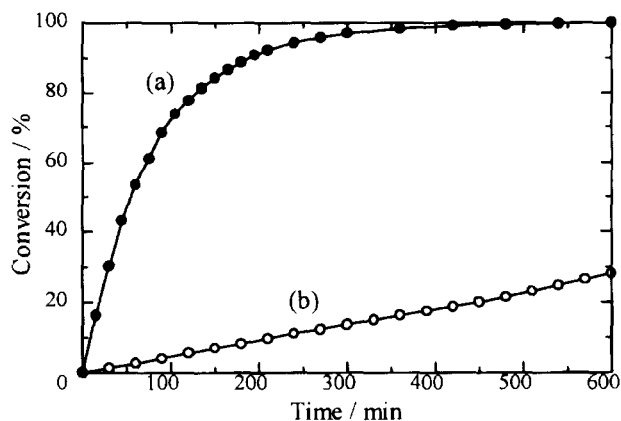


Fig. 6. Reactivity of (a) [Ni(3-EtOsAl-*meso*-stien)] and (b) [Ni(3-EtOsAl-*rac*-stien)] in dioxane. Conversion = 100 [Ni(3-EtOsAlton)]/[Ni(3-EtOsAl-*meso*-stien)] + [Ni(3-EtOsAlton)]}. [Ni(3-EtOsAlstien)] (0.057 g, 0.1 mmol) was dehydrogenated by 3 equiv amounts of DDQ (0.068, 0.3 mmol) in dioxane (100 ml) at 100 °C.

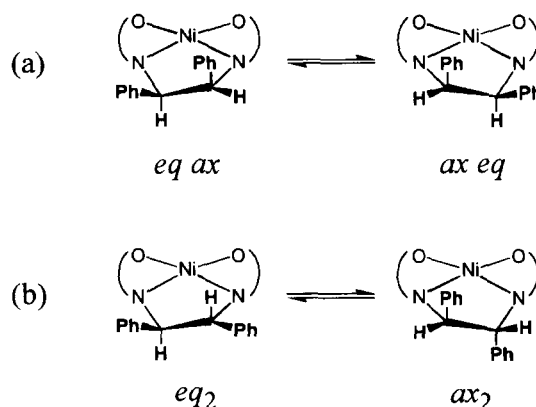


Fig. 7. Possible conformations of five-membered N–N chelate ring in (a) [Ni(3-EtOsAl-*meso*-stien)] and (b) [Ni(3-EtOsAl-*rac*-stien)].

groups in the *rac* complex, but are exposed to the oxidant in the *meso* complex. Therefore, the geometry of the *meso* complex is also preferable for dehydrogenation in solution.

The authors would like to thank to Prof. Masaaki Kojima of Okayama University and Prof. Kiyohiko Nakajima of Aichi University of Education for valuable discussions. We are also indebted to Ms. Makiko Yamakawa and Ms. Yukari Goto for their help in preparing the compounds. This work was supported in part by a Grant-in-Aid for Scientific Research No. 10640496 from the Ministry of Education, Science, Sports and Culture.

References

- 1 Y. N. Ito and T. Katsuki, *Bull. Chem. Soc. Jpn.*, **72**, 603 (1999).
- 2 a) K. Nakajima, M. Kojima, and J. Fujita, *Chem. Lett.*, **1986**, 1483. b) K. Yamamoto, E. Tsuchida, H. Nishide, M. Jikei, and K. Oyaizu, *Macromolecules*, **26**, 3432 (1993).
- 3 K. Nakajima, K. Kojima, M. Kojima, and J. Fujita, *Bull.*

Chem. Soc. Jpn., **63**, 2620 (1990).

4 G. Hoshina, M. Tsuchimoto, S. Ohba, K. Nakajima, H. Uekusa, Y. Ohashi, H. Ishida, and M. Kojima, *Inorg. Chem.*, **37**, 142 (1998).

5 "TEXSAN. Single Crystal Structure Analysis Software. Version 1.9. MSC, 3200 Research Forest Drive," Molecular Structure Corporation, The Woodlands, TX 77381, USA (1998).

6 G. M. Sheldrick, "SHELXL-97. Program for the Refinement of Crystal Structures," University of Göttingen, Germany (1997).

7 Red prismatic crystals of $[\text{Ni}(\text{3-MeOsalt})]\cdot\text{DDH}\cdot\text{CH}_3\text{-NO}_2\cdot\text{H}_2\text{O}$ were grown by slow evaporation of an acetonitrile solu-

tion. Crystal data: $\text{C}_{39}\text{H}_{31}\text{N}_5\text{Cl}_2\text{NiO}_9$, triclinic, $P\bar{1}$, $a = 12.682(1)$, $b = 13.983(2)$, $c = 12.206(3)$ Å, $\alpha = 112.70(1)$, $\beta = 98.25(1)$, $\gamma = 102.12(1)^\circ$, $V = 1890.9(6)$ Å³, $Z = 2$, $R = 0.113$ (disorder in DDH).

8 J. R. Zamian, E. R. Dockal, G. Castellano, and G. Oliva, *Polyhedron*, **14**, 2411 (1995).

9 R. Kasahara, M. Tsuchimoto, S. Ohba, K. Nakajima, and M. Kojima, *Inorg. Chem.*, **35**, 7661 (1996).

10 G. Hoshina, S. Ohba, K. Nakajima, H. Ishida, M. Kojima, and M. Tsuchimoto, *Bull. Chem. Soc. Jpn.*, **72**, 1037 (1999).
